

Time-reversal symmetry breaking and s -wave superconductivity in CaPd_2Ge_2 : A μSR studyV. K. Anand^{1,2,3,*} A. Bhattacharyya,^{4,†} D. T. Adroja^{5,6} K. Panda⁷ P. K. Biswas,^{5,**} A. D. Hillier,⁵ and B. Lake¹¹*Helmholtz-Zentrum Berlin für Materialien und Energie GmbH, Hahn-Meitner Platz 1, D-14109 Berlin, Germany*²*Department of Physics, University of Petroleum and Energy Studies, Dehradun 248007, Uttarakhand, India*³*Department of Mathematics and Physics, University of Stavanger, 4036 Stavanger, Norway*⁴*Department of Physics, Ramakrishna Mission Vivekananda Educational and Research Institute, Belur Math, Howrah 711202, West Bengal, India*⁵*ISIS Facility, Rutherford Appleton Laboratory, Chilton, Didcot, Oxon OX11 0QX, United Kingdom*⁶*Physics Department, Highly Correlated Matter Research Group, University of Johannesburg, P.O. Box 524, Auckland Park 2006, South Africa*⁷*Department of Physics, Ariel University, Ariel 40700*

(Received 10 February 2023; revised 10 November 2023; accepted 12 December 2023; published 28 December 2023)

CaPd_2Ge_2 which crystallizes in ThCr_2Si_2 -type body-centered tetragonal structure exhibits superconductivity below the critical temperature $T_c = 1.69$ K. We have investigated the superconducting gap structure and time-reversal symmetry of the ground state in CaPd_2Ge_2 by means of muon spin relaxation and rotation (μSR) measurements. Our analysis of μSR data collected in a transverse magnetic field reveals BCS superconductivity with a single-band s -wave singlet pairing and an isotropic energy gap having the value $2\Delta(0)/k_B T_c = 3.50(1)$. Further, an increased relaxation rate in zero-field μSR asymmetry spectra below T_c provides evidence for the presence of a spontaneous magnetic field in the superconducting state, revealing that the time-reversal symmetry is broken in CaPd_2Ge_2 .

DOI: [10.1103/PhysRevB.108.224519](https://doi.org/10.1103/PhysRevB.108.224519)**I. INTRODUCTION**

The 122-type compounds, owing to their simple ThCr_2Si_2 -type body-centered tetragonal (bct) structure, are of particular interest for the study of superconductivity. The FeAs-based 122 superconductors, such as $\text{Ba}(\text{K})\text{Fe}_2\text{As}_2$, are the well-known examples where superconductivity is achieved by suppressing the spin-density wave ordering of Fe moments [1–4]. Recently some of us investigated superconductivity in the ThCr_2Si_2 -type bct structured 122 compounds CaPd_2As_2 and CaPd_2Ge_2 [5,6]. CaPd_2As_2 exhibits superconductivity below $T_c = 1.27$ K [5]. The measured and derived superconducting state parameters characterize CaPd_2As_2 as a weakly coupled type II s -wave superconductor in the dirty limit [5]. However, despite a very sharp superconducting transition in single crystal CaPd_2As_2 , the jump in the electronic specific heat at T_c reflects a value of $\Delta C_e/\gamma_n T_c = 1.14$ which is much smaller than the BCS expected value of 1.43. The reason for the reduced value of $\Delta C_e/\gamma_n T_c$ is not clear.

A reduced value of $\Delta C_e/\gamma_n T_c = 1.21$ is also seen in the case of CaPd_2Ge_2 single crystal in which there is also a sharp and well-pronounced jump in the electronic specific heat at $T_c = 1.69$ K [6]. The superconducting-state electronic specific heat data have been analyzed by the α -model of BCS superconductivity [7,8]. For CaPd_2Ge_2 , the α -

model analysis yielded a value of $\alpha = \Delta(0)/k_B T_c = 1.62$ for $\Delta C_e/\gamma_n T_c = 1.21$ [6], which is lower than the BCS value $\alpha_{\text{BCS}} = 1.764$. For CaPd_2As_2 , a reduced value of $\alpha = 1.58$ was obtained for $\Delta C_e/\gamma_n T_c = 1.14$ [5]. The reduced value of $\Delta C_e/\gamma_n T_c$ and hence α may be caused by an anisotropic superconducting energy gap, or due to the presence of multiple superconducting gaps [8].

An *ab initio* calculation by the pseudopotential method and the generalized gradient approximation of density functional theory suggests that the major contribution to the density of states close to the Fermi level in CaPd_2Ge_2 comes from Pd d and Ge p orbitals [9]. Further, the estimate of electron-phonon interaction from the analysis of the Eliashberg spectral function supports the conventional mechanism for superconductivity in CaPd_2Ge_2 . The electron and phonon couple through the vibration of Pd and Ge atoms. The vibration of Pd and Ge atoms modifies the tetrahedral bond angles in PdGe_4 tetrahedra in such a way that the Pd d and Ge p orbitals overlap [9]. Such a change in tetrahedral bond angles in PdGe_4 and overlapping Pd d and Ge p orbitals is also seen in the Sr analog SrPd_2Ge_2 which exhibits superconductivity below 3 K [10].

With an objective of shedding light on the nature of the superconducting gap structure in CaPd_2Ge_2 , we decided to examine the superconducting gap structure by the microscopic muon spin relaxation and rotation (μSR) measurements. Herein, we present the results of our μSR study on CaPd_2Ge_2 . The analysis of the μSR data suggests a single-gap isotropic s -wave superconductivity in CaPd_2Ge_2 . However, to our great surprise, the μSR data reveals broken time-reversal symmetry

* vivekkranand@gmail.com

† amitava.bhattacharyya@rkmvu.ac.in

** Deceased.

(TRS) in the superconducting state of CaPd_2Ge_2 . A similar time-reversal symmetry-broken superconducting state was inferred from μSR investigations on $\text{Sc}_5\text{Co}_4\text{Si}_{10}$ [11] and other systems which also show an isotropic s -wave gap symmetry [12–14].

II. EXPERIMENTAL DETAILS

A polycrystalline sample of CaPd_2Ge_2 was prepared by the conventional solid-state reaction method using the high-purity starting materials (Ca-99.98%, Pd-99.95%, Ge-99.999% from Alfa Aesar) at the Core Lab for Quantum Materials, Helmholtz-Zentrum Berlin. The Pd and Ge powders along with the Ca pieces were pressed into a pellet and sealed inside a quartz tube with the pellet kept in an alumina crucible, which was then slowly heated to 800°C at a rate of 50°C per hour and kept there for 30 h, after which it was ground finely, again pelletized and sealed, and subsequently heat treated at 900°C for 72 h. This process of grinding, pelletizing, and sealing was repeated again, and the sample was heat treated at 900°C for another 72 h. The quality of the sample synthesized this way was checked by powder x-ray diffraction (XRD) at room temperature using $\text{Cu-K}\alpha$ radiation with the Bruker-D8 laboratory-based x-ray diffractometer. The XRD data (see Appendix, Fig. 4) revealed the desired phase and confirmed the ThCr_2Si_2 -type body-centered tetragonal structure of CaPd_2Ge_2 . The lattice parameters obtained from the refinement $a = b = 4.3271(2) \text{ \AA}$ and $c = 4.9823(7) \text{ \AA}$ and the c -axis position parameter $z_{\text{Ge}} = 0.376(7)$ are in good agreement with the respective values obtained for single crystal CaPd_2Ge_2 [6] and with the literature values [15].

The μSR measurements were carried out at the ISIS facility of the Rutherford Appleton Laboratory, Didcot, United Kingdom, using the muon spectrometer MuSR which has 64 detectors for transverse and longitudinal applied field directions [16]. The CaPd_2Ge_2 powder sample was mounted on a high-purity Ag plate (99.999%). The use of Ag minimizes the contribution from the sample holder as the Ag gives only a nonrelaxing signal. The powdered sample was mounted to the Ag plate by applying the diluted GE varnish which was then covered with thin silver foils. As muons are very sensitive to magnetic fields, correction coils were used to neutralize the stray fields to within $1 \mu\text{T}$. μSR data were collected in both the zero field (ZF) and the applied transverse field (TF). The ZF μSR measurements were made at several temperatures between 0.1 and 2.5 K. The TF μSR measurements were carried out between 0.1 and 2.5 K in the presence of transverse fields of $H = 10, 20, 30,$ and 40 mT , which lie in between the lower critical field $H_{c1} = 3.1 \text{ mT}$ and the upper critical field $H_{c2} = 134 \text{ mT}$ [6]. In the superconducting state with the field-cooled mode, muons probe the vortex lattice state. The μSR spectra were analyzed with the program WIMDA [17].

III. RESULTS AND DISCUSSION

A. ZF μSR : Time-reversal symmetry state

Figure 1(a) presents the representative μSR data collected in the zero field at 0.1 K (which is well below T_c) and 2.5 K (which is well above T_c). The ZF μSR spectra allow us to discern the time-reversal symmetry state of CaPd_2Ge_2 by

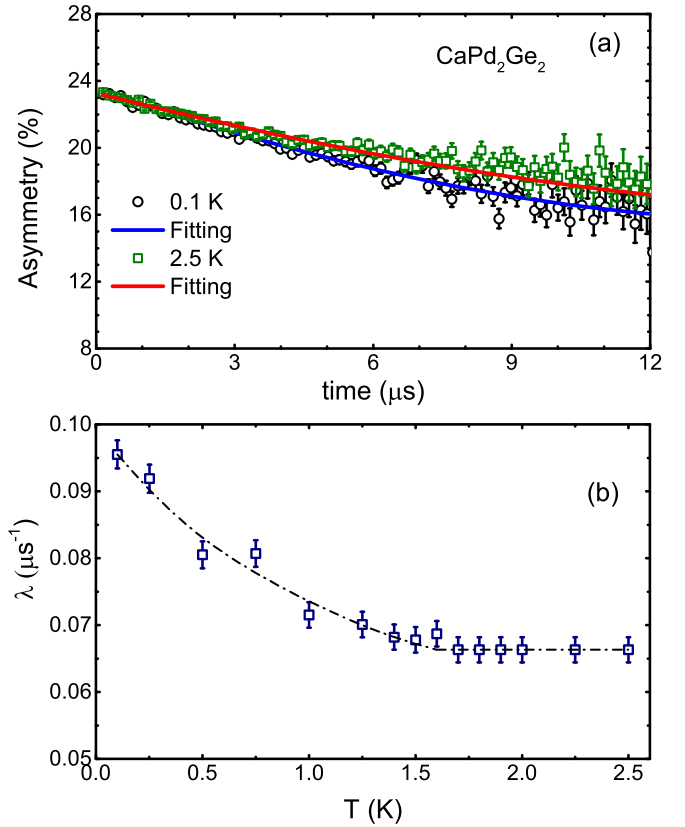


FIG. 1. (a) Zero field μSR time spectra for CaPd_2Ge_2 collected at 0.1 and 2.5 K. The solid curves represent the fit according to Eq. (1). (b) The temperature T dependence of the muon spin relaxation rate λ_{ZF} obtained from the fits μSR spectra collected at various T . The dashed navy blue line is the guide to the eye.

detecting the extremely weak magnetic field associated with the breaking of time-reversal symmetry. The time t evolution of muon spin asymmetry spectra in the zero field can be modeled by a damped Gaussian Kubo-Toyabe function [18,19],

$$A_{\text{ZF}}(t) = A_0 G_{\text{KT}}(t) e^{-\lambda_{\text{ZF}} t} + A_{\text{BG}}, \quad (1)$$

where A_0 is the initial muon asymmetry in the zero field,

$$G_{\text{KT}}(t) = \left[\frac{1}{3} + \frac{2}{3} (1 - \sigma_{\text{KT}}^2 t^2) e^{-\sigma_{\text{KT}}^2 t^2 / 2} \right] \quad (2)$$

is the Gaussian Kubo-Toyabe function, λ_{ZF} is the muon relaxation rate associated with the fluctuating fields due to electronic moments, and A_{BG} is the time-independent contribution from the sample holder. In Eq. (2), the parameter σ_{KT} accounts for the Gaussian distribution of static fields associated with the nuclear moments. σ_{KT} is related to the local field distribution width as $H_\mu = \sigma_{\text{KT}} / \gamma_\mu$, where γ_μ is the muon gyromagnetic ratio, $\gamma_\mu / 2\pi = 135.53 \text{ MHz/T}$.

The representative fits of μSR spectra by the damped Gaussian Kubo-Toyabe function [Eq. (1)] are shown by solid curves in Fig. 1(a). The λ_{ZF} values obtained from the fits of μSR spectra over the temperature range 0.1 K to 2.5 K are shown in Fig. 1(b). The T dependence of σ_{KT} obtained from the fitting is presented in the Appendix [Fig. 5(a)]. At $T > T_c$, $\sigma_{\text{KT}} \approx 0.0703 \mu\text{s}^{-1}$ and is nearly temperature independent over 0.1 to 2.5 K. As can be seen from Fig. 1(b), there is

an increase in λ_{ZF} at $T < T_c$. This kind of increase in λ_{ZF} indicates that the muons detect a spontaneous internal field while entering the superconducting state. Thus, the zero-field μ SR measurements reveal that the time-reversal symmetry in the superconducting state is not preserved, and hence there is a time-reversal symmetry breaking in CaPd_2Ge_2 . The $\lambda_{ZF}(T)$ seems to have an upward concavity which is not usual. Most of the superconductors with the TRS broken superconducting state have been found to show a downward concavity in $\lambda_{ZF}(T)$. The origin for this unusual upward concavity is not clear. An upward concavity in $\lambda_{ZF}(T)$ was also observed in the case of fully gapped s -wave superconductor ScS with the time-reversal symmetry broken superconducting state [14].

Below T_c , $\Delta\lambda_{ZF}$ increases by $0.029(1) \mu\text{s}^{-1}$, corresponding to a characteristic magnetic field strength $\Delta\lambda_{ZF}/\gamma_\mu = 0.034(2) \text{mT}$, which provides clear evidence for the time-reversal symmetry breaking in the superconducting state of CaPd_2Ge_2 . Muon spin relaxation studies have provided evidence of TRS breaking in several superconducting materials like Sr_2RuO_4 with a possible chiral p -wave symmetry [20–22]; SrPtAs with a chiral d -wave symmetry [23]; LaNiC_2 with two nodeless gaps [24]; and $\text{A}_3\text{Rh}_6\text{Sn}_{18}$ ($A = \text{Y, R, or Sc}$) [25–27], $\text{La}_7(\text{Ir, Rh, Pd})_3$ [12,13,28], and Zr_3Ir [29] with an s -wave gap symmetry. For the present compound the spontaneous flux density due to superconductivity as estimated using the change in ZF- μ SR relaxation rate above is $0.034(2) \text{mT}$. A similar estimate for Sr_2RuO_4 shows the appearance of a characteristic field of 0.050mT [20]. The spontaneous field associated with TRS breaking in the superconducting state of La_7Pd_3 has been found to be 0.006mT [28] and that for Zr_3Ir has been found to be 0.009mT [29].

Recently, we found evidence for TRS breaking in the centrosymmetric superconductor $\text{Sc}_5\text{Co}_4\text{Si}_{10}$, for which also an isotropic fully gapped s -wave symmetry has been inferred from the μ SR study [11]. The TRS breaking is usually associated with a nonunitary triplet pairing state or a mixed singlet-triplet state. However, a group theoretical analysis of Ginzburg-Landau's free energy and symmetry allowed pairing states using density functional theory does not support the presence of either a nonunitary triplet pairing state or a mixed singlet-triplet state in $\text{Sc}_5\text{Co}_4\text{Si}_{10}$ [11]. Accordingly, it was proposed that the Fermi surface topography of $\text{Sc}_5\text{Co}_4\text{Si}_{10}$ may allow TRS breaking by conventional electron-phonon mechanism [11]. We are under the impression that a similar physics associated with the Fermi surface topography could be held responsible for the observation of TRS breaking in the superconducting state of CaPd_2Ge_2 with a fully gapped s -wave symmetry.

Another mechanism which has been proposed for the TRS breaking in fully gap single-band BCS superconductors is based on loop supercurrent order applicable to the systems having complex crystal symmetry that allows the formation of microscopic supercurrent loops, such as in Re_6X ($X = \text{Zr, Hf, and Ti}$) [30,31]. Ghosh *et al.* [31] proposed that if the lattice unit cell of a superconducting material consists of more than two distinct symmetry-related sites, and the symmetry allows the order parameter to have different amplitude and phase at these symmetry sites, then it is possible to realize a superconducting ground state with spontaneous microscopic Josephson currents flowing between these symmetry sites of

unit cells. These microscopic Josephson currents are termed as supercurrent loops, which, in turn, produce a weak static magnetic field that can break the time-reversal symmetry and can be probed by μ SR measurement, which is extremely sensitive to the presence of even very weak magnetic field. On the other hand, within the BCS formalism a TRS breaking in a multiband superconductor can be associated with the development of a complex gap structure on account of the interband interactions [32].

B. TF μ SR: Superconducting gap structure

Figure 2 presents the transverse-field μ SR asymmetry time spectra at 2.5K (above T_c) and 0.1K (below T_c) along with their Fourier transforms. The TF μ SR data were collected in a field-cooled mode in the presence of applied magnetic fields of 10 and 30mT . It is clear from Figs. 2(a) and 2(e) that in the superconducting state ($T < T_c$) the μ SR spectra depolarize strongly on account of the inhomogeneous field distribution in the vortex state.

The TF μ SR spectra could be fitted by a Gaussian oscillatory function and an oscillatory background [33–35]:

$$A_{\text{TF}}(t) = A_1 \cos(\omega t + \phi) e^{-\sigma_{\text{TF}}^2 t^2 / 2} + A_{\text{BG}} \cos(\omega_{\text{BG}} t + \phi), \quad (3)$$

where A_1 is the initial asymmetry of the sample and A_{BG} that of the silver sample holder; $\omega = \gamma_\mu H_{\text{int}}$, H_{int} being the internal field at the muon site; $\omega_{\text{BG}} = \gamma_\mu H_{\text{int,BG}}$; and ϕ is the initial phase offset of the muon precession signal. σ_{TF} is the Gaussian relaxation rate that can be expressed as $\sigma_{\text{TF}}^2 = \sigma_{\text{sc}}^2 + \sigma_{\text{nm}}^2$, where σ_{sc} accounts for the inhomogeneous field variation across the superconducting vortex lattice, and σ_{nm} is the contribution due to the nuclear dipolar moments. σ_{nm} was determined by fitting the spectra at $T > T_c$ and kept fixed for $T < T_c$, i.e., in the superconducting state, to obtain the value of σ_{sc} from the fit parameter σ_{TF} .

The representative fits of the TF μ SR spectra by the function discussed above in Eq. (3) are shown by solid red curves in Figs. 2(a), 2(b), 2(e), and 2(f). The value of σ_{TF} is found to be much larger at $T < T_c$ (superconducting state) than that at $T > T_c$ (normal state) [see Appendix, Fig. 5(b)]. Further, the fitting of TF μ SR spectra at 0.1K and 10mT by Eq. (3) reveals that A_1 is 0.887 and A_{BG} is 0.113 of the total initial asymmetry, thus giving us an estimate of the lower bound of the superconducting volume fraction of 88.7% . This confirms the occurrence of bulk superconductivity in CaPd_2Ge_2 as also inferred from the previous study [6].

The magnetic field probability distribution determined by the maximum entropy method is shown in Figs. 2(c), 2(d), 2(g), and 2(h) corresponding to the TF μ SR spectra in Figs. 2(a), 2(b), 2(e), and 2(f), respectively. As can be seen from Figs. 2(d) and 2(h), at 2.5K (in normal state) there is only one sharp peak at a value of H_{int} equal to the applied H . On the other hand, at 0.1K (in the superconducting state), there is another broad peak at H_{int} lower than the applied H in addition to the one at the applied H [see Figs. 2(c) and 2(g)]. Such an appearance of an additional peak is a characteristic of type II superconductivity. This inference of a type II behavior

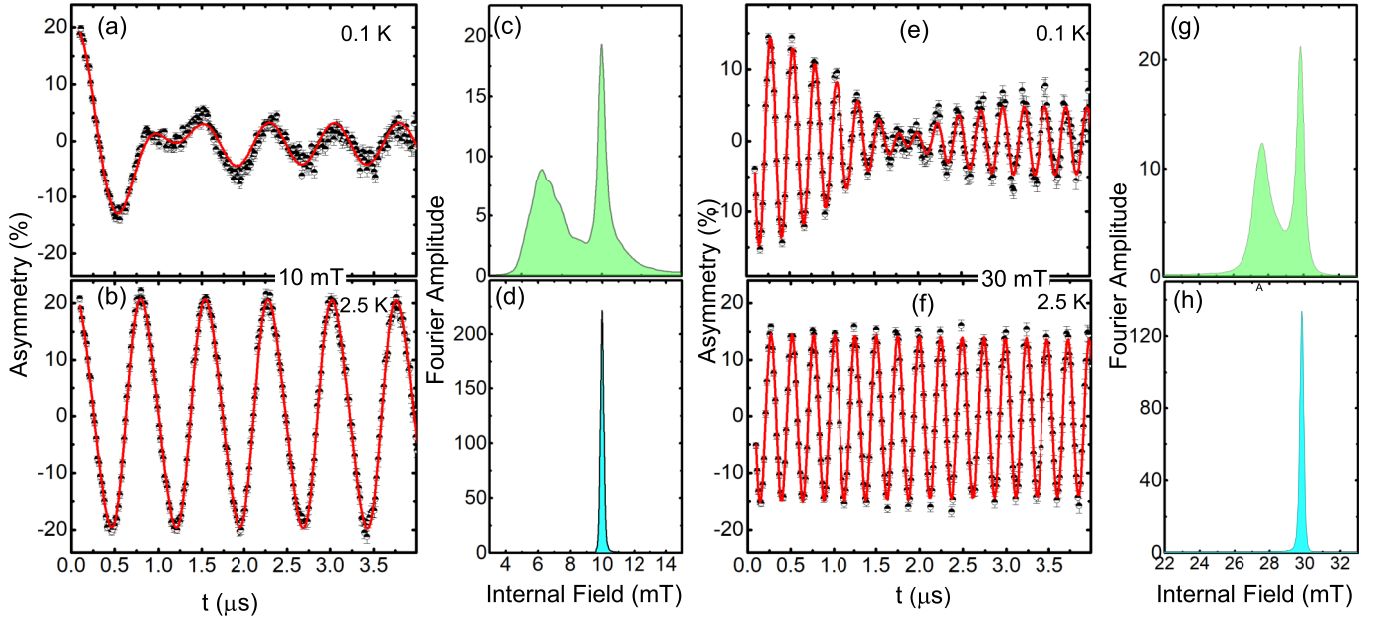


FIG. 2. Transverse field μ SR time spectra for CaPd_2Ge_2 collected in the field-cooled state in an applied magnetic field of 10 mT at (a) 0.1 K and (b) 2.5 K, and that in a field of 30 mT at (e) 0.1 K and (f) 2.5 K along with their corresponding Fourier-transformed maximum entropy spectra in panels (c), (d), (g), and (h), respectively. The solid red curve represents the fit according to Eq. (3).

in CaPd_2Ge_2 is consistent with the estimated value of the Ginzburg-Landau parameter ($\kappa_{\text{GL}} = 6.3 > 1/\sqrt{2}$) [6].

The T dependence of σ_{sc} extracted from the values of σ_{TF} that were obtained from the fit of the TF μ SR spectra is shown in Fig. 3(a). The H dependence of σ_{sc} is shown in Fig. 3(b). As the TF μ SR spectra were collected at fields much lower than the upper critical field H_{c2} , the Brandt [36–38] relation

$$\sigma_{\text{sc}} = \frac{4.83 \times 10^4}{\lambda_{\text{eff}}^2} (1 - H_{\text{ext}}/H_{c2}) \times [1 + 1.21(1 - \sqrt{(H_{\text{ext}}/H_{c2})})^3], \quad (4)$$

which holds good for $H/H_{c2} \leq 0.25$, and for $\kappa_{\text{GL}} \geq 5$, can be used to estimate the effective penetration depth λ_{eff} . In this relation, σ_{sc} is in units of μs^{-1} and λ_{eff} is in nanometers. For

CaPd_2Ge_2 , $\kappa_{\text{GL}} = 6.3$ and $H_{c2} = 134$ mT [6]; therefore, we can use the above Brandt relation [Eq. (4)] to estimate the λ_{eff} . The T dependence of λ_{eff} obtained this way is plotted as $\lambda_{\text{eff}}^{-2}(T)/\lambda_{\text{eff}}^{-2}(0)$ in Fig. 3(c).

Apart from the information about the magnetic penetration depth, σ_{sc} also provides information about the superfluid density and size, as well as the symmetry of the superconducting energy gap. In order to obtain information about the superconducting gap structure we analyzed $\lambda_{\text{eff}}^{-2}(T)/\lambda_{\text{eff}}^{-2}(0)$ by [39,40]

$$\frac{\sigma_{\text{sc}}(T)}{\sigma_{\text{sc}}(0)} = \frac{\lambda_{\text{eff}}^{-2}(T, \Delta)}{\lambda_{\text{eff}}^{-2}(0)} = 1 + \frac{1}{\pi} \int_0^{2\pi} \int_{\Delta(T, \varphi)}^{\infty} \frac{\partial f}{\partial E} \frac{E dE d\varphi}{\sqrt{E^2 - \Delta^2(T, \varphi)}}, \quad (5)$$

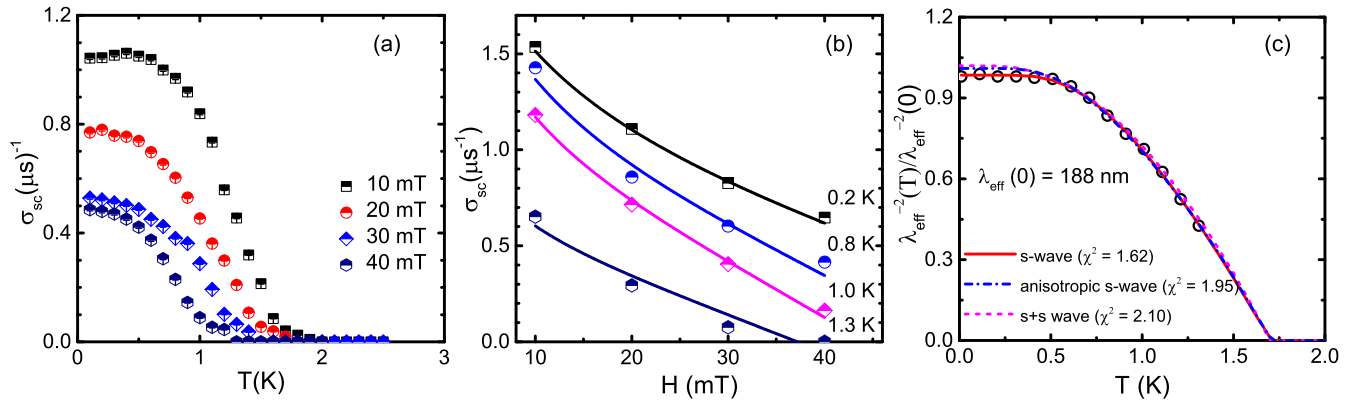


FIG. 3. (a) Temperature T dependence of the muon spin relaxation rate σ_{sc} for CaPd_2Ge_2 collected in various applied transverse magnetic fields H in the field-cooled state. (b) H dependence of σ_{sc} at indicated temperatures. The solid lines are the fits according to Eq. (4). (c) T dependence of the inverse square of the normalized penetration depth λ_{eff} . The solid curve represents the fit for an isotropic single-gap s -wave model according to Eq. (5).

TABLE I. Fitting parameters obtained from the analysis of $\lambda_{\text{eff}}^{-2}(T)/\lambda_{\text{eff}}^{-2}(0)$ for CaPd_2Ge_2 according to Eq. (5) using three models: The isotropic s -wave model, the anisotropic s -wave model, and the $s + s$ -wave model.

Model	$\Delta_i(0)$ (meV)	$2\Delta_i(0)/k_B T_C$	χ^2
Isotropic s -wave	0.252(3)	3.50(4)	1.62(2)
Anisotropic s -wave	0.311(4)	4.32(6)	1.95(4)
Two gap $s + s$ -wave	0.281(2), 0.124(5)	3.90(1), 1.72(5)	2.10(6)

where f is the Fermi function and φ is the azimuthal angle in the direction of the Fermi surface. The Fermi function is given by $f = [1 + \exp(E/k_B T)]^{-1}$. The T and φ dependence of the order parameter $\Delta(T, \varphi)$ is given by $\Delta(T, \varphi) = \Delta(0)\delta(T/T_C)g(\varphi)$ [41,42]. The angular dependence of the superconducting gap is contained in the function $g(\varphi)$. For s -wave BCS superconductivity with an isotropic gap, $g(\varphi) = 1$ [41,42]. Further, for the case of BCS superconductivity, $\delta(T/T_C) = \tanh\{(1.82)[1.018(T_C/T - 1)]^{0.51}\}$ [43].

In order to determine the superconducting gap structure of CaPd_2Ge_2 , we analyzed the T dependence of $\lambda_{\text{eff}}^{-2}(T)/\lambda_{\text{eff}}^{-2}(0)$ by Eq. (5) using three models: The isotropic s -wave model, the anisotropic s -wave model, and the $s + s$ -wave model. For the $s + s$ -wave model, both the energy gaps were taken to be isotropic, and both the gaps were allowed to vary freely without any constraint. The fits for the three models are shown in Fig. 3(c) and the fitting parameters are listed in Table I. It is evident from the fits in Fig. 3(c), as well as from the values of the quality of the fit parameter χ^2 in Table I, that the single-gap isotropic s -wave model describes the $\lambda_{\text{eff}}(T)$ data better than the anisotropic s -wave model and/or the two-gap $s + s$ -wave model.

The single-gap isotropic s -wave model analysis, which describes the T dependence of λ_{eff} the best, yielded an energy gap of $\Delta(0) = 0.25$ meV which corresponds to $2\Delta(0)/k_B T_C = 3.50(1)$. This value is quite close to the expected BCS weak-coupling superconductor value of 3.53 but a little higher than the value 3.24 obtained from the jump in specific heat at the superconducting transition [6]. In addition, the s -wave analysis of $\lambda_{\text{eff}}^{-2}(T)/\lambda_{\text{eff}}^{-2}(0)$ provides an estimate of $\lambda_{\text{eff}}(0) = 188(2)$ nm, which is consistent with the previous estimate of $\lambda_{\text{eff}}(0) = 186(16)$ nm from the penetration depth measurement using the tunnel diode resonator [6]. In order to estimate the λ_{eff} according to Eqs. (4) and (5) we fitted the σ_{sc} values obtained from all the applied transverse fields. Further, following the approach detailed in Refs. [44–46], and assuming that approximately all the normal state carriers (n_e) contribute to the superconductivity (i.e., $n_s \approx n_e$), we have estimated the superconducting carrier density n_s . Using the relation $n_s = m^* c^2 / 4\pi \lambda_{\text{eff}}(0) e^2$, for $\lambda_{\text{eff}}(0) = 188(2)$ nm, we obtained $n_s = 1.20(1) \times 10^{27}$ carriers m^{-3} , where we used the value of the effective mass $m^* = (1 + \lambda_{e\text{-ph}})m_e \approx 1.51 m_e$, with the electron-phonon coupling constant $\lambda_{e\text{-ph}} \approx 0.51$ as estimated in Ref. [6] according to McMillan's relation [47] and m_e being the free-electron mass.

Next we estimate the Fermi temperature T_F using the relation [48]

$$k_B T_F = \frac{\hbar^2}{2m^*} (3\pi^2 n_s)^{2/3}, \quad (6)$$

which, for $n_s = 1.20(1) \times 10^{27}$ carriers m^{-3} , gives $T_F = 3164$ K. This in turn gives the ratio $T_c/T_F \approx 0.0005$ and hence characterizes CaPd_2Ge_2 as a conventional superconductor based on the Uemura plot [49,50] that provides an empirical relation between T_c and T_F to classify a superconductor into the categories of conventional and unconventional superconductors. Uemura *et al.* [49,50] plotted the values of the ratio T_c/T_F for many conventional and unconventional superconductors and suggested that an unconventional and exotic superconductivity is observed for those superconductors for which $0.01 \leq T_c/T_F \leq 0.1$, whereas for a conventional superconductor $T_c/T_F \leq 0.001$. The value $T_c/T_F \approx 0.0005$ for CaPd_2Ge_2 indeed falls in the range of a conventional superconductor. Therefore, the time-reversal symmetry breaking in CaPd_2Ge_2 is conjectured to have different physics than the one applicable to multiband or unconventional superconductors, or the systems with multiorbital character of states at the Fermi level.

IV. CONCLUSIONS

We have probed the superconducting gap structure and the time-reversal symmetry state of superconducting CaPd_2Ge_2 through the muon spin relaxation and rotation measurements in both the zero field and the transverse magnetic field. The TF μ SR spectra were analyzed by a Gaussian oscillatory function, and the temperature and field dependencies of the muon spin depolarization rate associated with the superconducting state σ_{sc} were obtained. Further, we obtained the magnetic penetration depth from $\sigma_{\text{sc}}(T)$. Information about the energy gap and pairing symmetry was obtained from the analysis of $\lambda_{\text{eff}}(T)$. $\lambda_{\text{eff}}(T)$ is well described by the single-band s -wave model, indicating an isotropic superconducting gap structure. An energy gap of $2\Delta(0)/k_B T_C = 3.50(1)$ is obtained from the analysis. On the other hand, the analysis of ZF μ SR spectra revealed an increased relaxation rate below T_c on account of the spontaneous magnetic field associated with time-reversal symmetry breaking in CaPd_2Ge_2 . The observation of time-reversal symmetry breaking in CaPd_2Ge_2 is quite striking and invites further experimental and theoretical investigations to understand the origin of this unconventional feature despite the conventional single-band isotropic s -wave singlet pairing symmetry of the superconducting order parameter in this compound.

ACKNOWLEDGMENTS

A.B. thanks the Science & Engineering Research Board for a CRG Research (Grant No. CRG/2020/000698). D.T.A. thanks the Royal Society of London for the Newton Advanced Fellowship Funding between the United Kingdom and China, and the International Exchange funding between the United Kingdom and Japan. D.T.A. also thanks EPSRC UK (Grant No. EP/W00562X/1) for funding. We thank the ISIS Facility for providing beam time RB1510100 [51].

APPENDIX

Figure 4 shows the powder x-ray diffraction pattern of CaPd_2Ge_2 collected at room temperature along with

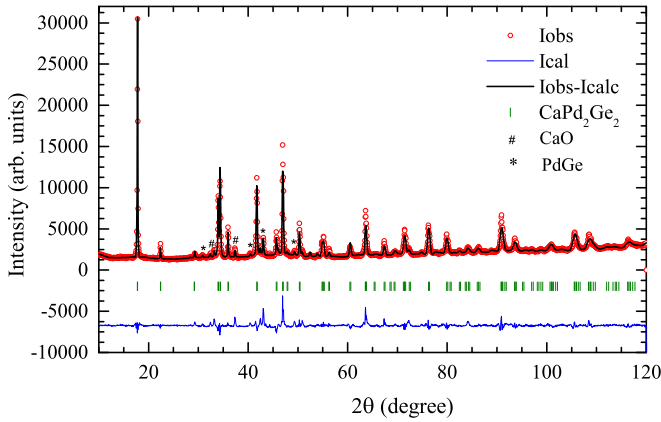


FIG. 4. Room-temperature powder x-ray diffraction pattern (Cu- K_{α} radiation) of CaPd_2Ge_2 along with the Rietveld refinement profile. The Rietveld refinement shown by the solid black curve represents a major contribution from the bulk CaPd_2Ge_2 . The Bragg peak positions for CaPd_2Ge_2 are shown by the short vertical bars. The differences between the experimental and calculated intensities are shown by the lowermost blue curves. The impurity peaks marked with * and # represent the PdGe and CaO impurities, respectively.

the Rietveld refinement profile. The refinement confirmed the ThCr_2Si_2 -type body-centered tetragonal structure of CaPd_2Ge_2 . We also see a few impurity peaks from PdGe and CaO, marked with * and #, respectively, in Fig. 4. We estimate about 2% CaO and 6% PdGe, altogether about 8% impurities in the present sample. The impurities are nonmagnetic in nature and therefore do not affect the results presented on the superconducting properties of CaPd_2Ge_2 . The contribution from such a spurious non-superconducting phase to μSR , if any, should be noticeable only in applied fields and not in the zero field.

Figure 5(a) shows the temperature dependence of the Kubo-Toyabe depolarization rate σ_{KT} obtained from the fitting of zero-field μSR spectra of CaPd_2Ge_2 by Eq. (1). σ_{KT} remains constant with a value of $\approx 0.0703 \mu\text{s}^{-1}$. Figure 5(b) shows the temperature dependence of the Gaussian relaxation rate σ_{TF} obtained from the fitting of

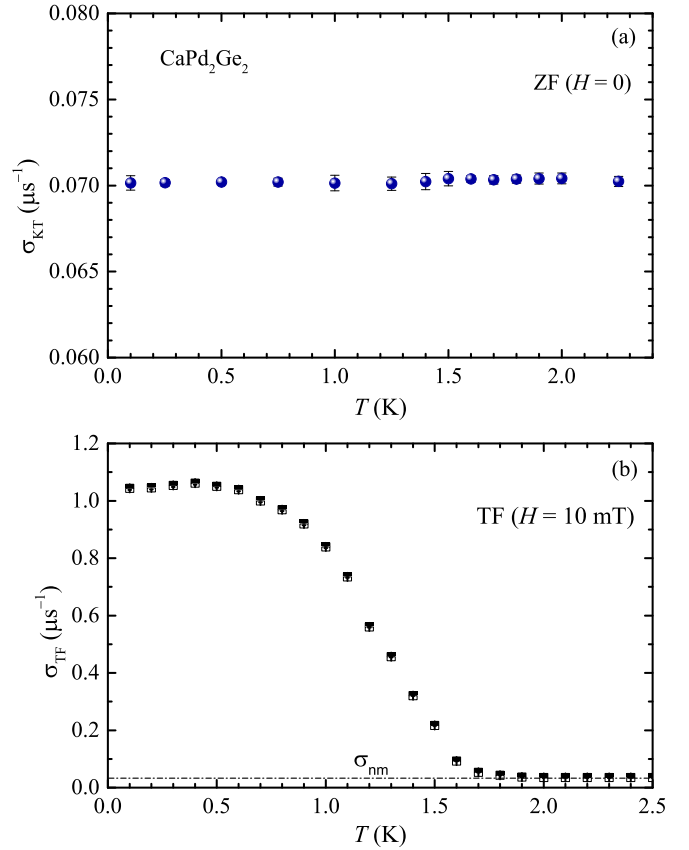


FIG. 5. (a) The temperature T dependence of the Kubo-Toyabe depolarization rate σ_{KT} obtained from the fitting of zero-field (ZF) μSR spectra of CaPd_2Ge_2 by Eq. (1). (b) The T dependence of the Gaussian relaxation rate σ_{TF} obtained from the fitting of transverse-field (TF) μSR spectra measured in the applied field $H = 10 \text{ mT}$ by Eq. (3). σ_{nm} represents the contribution due to the nuclear dipolar moments.

transverse-field μSR spectra (for $H = 10 \text{ mT}$) by Eq. (3). The contribution due to the nuclear dipolar moments is also shown in Fig. 5(b). We find $\sigma_{\text{nm}} \approx 0.0354 \mu\text{s}^{-1}$ at T above T_c .

[1] D. C. Johnston, *Adv. Phys.* **59**, 803 (2010).
 [2] G. R. Stewart, *Rev. Mod. Phys.* **83**, 1589 (2011).
 [3] J. Chen, M. B. Gamza, J. Banda, K. Murphy, J. Tarrant, M. Brando, and F. M. Grosche, *Phys. Rev. Lett.* **125**, 237002 (2020).
 [4] J. Baglo, J. Chen, K. Murphy, R. Leenen, A. McCollam, M. L. Sutherland, and F. M. Grosche, *Phys. Rev. Lett.* **129**, 046402 (2022).
 [5] V. K. Anand, H. Kim, M. A. Tanatar, R. Prozorov, and D. C. Johnston, *Phys. Rev. B* **87**, 224510 (2013).
 [6] V. Anand, H. Kim, M. A. Tanatar, R. Prozorov, and D. C. Johnston, *J. Phys.: Condens. Matter* **26**, 405702 (2014).
 [7] H. Padamsee, J. Neighbor, and C. Shiffman, *J. Low Temp. Phys.* **12**, 387 (1973).
 [8] D. C. Johnston, *Supercond. Sci. Technol.* **26**, 115011 (2013).

[9] E. Karaca, E. Arslan, H. M. Tütüncü, and G. Srivastava, *Philos. Mag.* **97**, 1866 (2017).
 [10] E. Karaca, H. M. Tütüncü, H. Y. Uzunok, G. P. Srivastava, and Ş. Uğur, *Phys. Rev. B* **93**, 054506 (2016).
 [11] A. Bhattacharyya, M. R. Lees, K. Panda, P. P. Ferreira, T. T. Dorini, E. Gaudry, L. T. F. Eleno, V. K. Anand, J. Sannigrahi, P. K. Biswas, R. Tripathi, and D. T. Adroja, *Phys. Rev. Mater.* **6**, 064802 (2022).
 [12] D. Singh, M. S. Scheurer, A. D. Hillier, D. T. Adroja, and R. P. Singh, *Phys. Rev. B* **102**, 134511 (2020).
 [13] J. A. T. Barker, D. Singh, A. Thamizhavel, A. D. Hillier, M. R. Lees, G. Balakrishnan, D. M. Paul, and R. P. Singh, *Phys. Rev. Lett.* **115**, 267001 (2015).
 [14] Arushi, R. K. Kushwaha, D. Singh, A. D. Hillier, M. S. Scheurer, and R. P. Singh, *Phys. Rev. B* **106**, L020504 (2022).

- [15] G. Venturini, B. Malaman, and B. Roques, *J. Solid State Chem.* **79**, 136 (1989).
- [16] Muon Science: Muons in Physics, Chemistry and Materials, edited by S. L. Lee, S. H. Kilcoyne, and R. Cywinski, in *Proceedings of the Fifty First Scottish Universities Summer School in Physics* (Taylor & Francis Group, New York, 1999).
- [17] F. Pratt, *Phys. B: Condens. Matter* **289-290**, 710 (2000).
- [18] A. Bhattacharyya, D. T. Adroja, J. S. Lord, L. Wang, Y. Shi, K. Panda, H. Luo, and A. M. Strydom, *Phys. Rev. B* **101**, 214437 (2020).
- [19] A. Bhattacharyya, K. Panda, D. Adroja, N. Kase, P. Biswas, S. Saha, T. Das, M. Lees, and A. Hillier, *J. Phys.: Condens. Matter* **32**, 085601 (2020).
- [20] G. M. Luke, Y. Fudamoto, K. M. Kojima, M. I. Larkin, J. Merrin, B. Nachumi, Y. J. Uemura, Y. Maeno, Z. Q. Mao, Y. Mori, H. Nakamura, and M. Sigrist, *Nature (London)* **394**, 558 (1998).
- [21] G. M. Luke, Y. Fudamoto, K. M. Kojima, M. I. Larkin, B. Nachumi, Y. J. Uemura, J. E. Sonier, Y. Maeno, Z. Q. Mao, Y. Mori *et al.*, *Phys. B: Condens. Matter* **289-290**, 373 (2000).
- [22] V. Grinenko, S. Ghosh, R. Sarkar, J.-C. Orain, A. Nikitin, M. Elender, D. Das, Z. Guguchia, F. Brückner, M. E. Barber *et al.*, *Nat. Phys.* **17**, 748 (2021).
- [23] P. K. Biswas, H. Luetkens, T. Neupert, T. Stürzer, C. Baines, G. Pascua, A. P. Schnyder, M. H. Fischer, J. Goryo, M. R. Lees, H. Maeter, F. Brückner, H.-H. Klauss, M. Nicklas, P. J. Baker, A. D. Hillier, M. Sigrist, A. Amato, and D. Johrendt, *Phys. Rev. B* **87**, 180503(R) (2013).
- [24] A. D. Hillier, J. Quintanilla, and R. Cywinski, *Phys. Rev. Lett.* **102**, 117007 (2009).
- [25] A. Bhattacharyya, D. T. Adroja, N. Kase, A. D. Hillier, A. M. Strydom, and J. Akimitsu, *Phys. Rev. B* **98**, 024511 (2018).
- [26] A. Bhattacharyya, D. Adroja, N. Kase, A. Hillier, J. Akimitsu, and A. Strydom, *Sci. Rep.* **5**, 12926 (2015).
- [27] A. Bhattacharyya, D. T. Adroja, J. Quintanilla, A. D. Hillier, N. Kase, A. M. Strydom, and J. Akimitsu, *Phys. Rev. B* **91**, 060503(R) (2015).
- [28] D. A. Mayoh, A. D. Hillier, G. Balakrishnan, and M. R. Lees, *Phys. Rev. B* **103**, 024507 (2021).
- [29] T. Shang, S. K. Ghosh, J. Z. Zhao, L.-J. Chang, C. Baines, M. K. Lee, D. J. Gawryluk, M. Shi, M. Medarde, J. Quintanilla, and T. Shiroka, *Phys. Rev. B* **102**, 020503(R) (2020).
- [30] S. K. Ghosh, M. Smidman, T. Shang, J. F. Annett, A. D. Hillier, J. Quintanilla, and H. Yuan, *J. Phys.: Condens. Matter* **33**, 033001 (2021).
- [31] S. K. Ghosh, J. F. Annett, and J. Quintanilla, *New J. Phys.* **23**, 083018 (2021).
- [32] B. J. Wilson and M. P. Das, *J. Phys.: Condens. Matter* **25**, 425702 (2013).
- [33] D. T. Adroja, A. Bhattacharyya, Y. J. Sato, M. R. Lees, P. K. Biswas, K. Panda, V. K. Anand, G. B. G. Stenning, A. D. Hillier, and D. Aoki, *Phys. Rev. B* **103**, 104514 (2021).
- [34] A. Bhattacharyya, D. T. Adroja, K. Panda, S. Saha, T. Das, A. J. S. Machado, O. V. Cigarroa, T. W. Grant, Z. Fisk, A. D. Hillier, and P. Manfrinetti, *Phys. Rev. Lett.* **122**, 147001 (2019).
- [35] A comparison of Eqs. (1) and (3) reveals that the exponential multiplier of the ZF fitting function is not required for the case of the TF fitting function. This can be understood as follows: in TF measurements, the externally applied field is dominant and effectively suppresses the impact of any intrinsic or external fluctuating fields as well as Kubo-Toyabe contribution. Therefore, the exponential contribution, which accounts for the effects of fluctuating fields, which is very small, of the order of μT , becomes less relevant under the strong influence of the transverse field. For the present compound, the fluctuating field of 0.034(2) mT estimated from the change in the ZF- μSR relaxation rate is much smaller than the applied TFs of 10 and 30 mT. For this reason, the multiplication by the exponential term can be neglected for TF fitting.
- [36] E. Brandt, *J. Low Temp. Phys.* **73**, 355 (1988).
- [37] E. H. Brandt, *Phys. Rev. B* **68**, 054506 (2003).
- [38] K. Panda, A. Bhattacharyya, D. T. Adroja, N. Kase, P. K. Biswas, S. Saha, T. Das, M. R. Lees, and A. D. Hillier, *Phys. Rev. B* **99**, 174513 (2019).
- [39] R. Prozorov and R. W. Giannetta, *Supercond. Sci. Technol.* **19**, R41 (2006).
- [40] A. Bhattacharyya, P. P. Ferreira, K. Panda, S. H. Masunaga, L. R. de Faria, L. E. Correa, F. B. Santos, D. T. Adroja, K. Yokoyama, T. T. Dorini, R. F. Jardim, L. T. F. Eleno, and A. J. S. Machado, *J. Phys.: Condens. Matter* **34**, 035602 (2022).
- [41] J. F. Annett, *Adv. Phys.* **39**, 83 (1990).
- [42] G. M. Pang, M. Smidman, W. B. Jiang, J. K. Bao, Z. F. Weng, Y. F. Wang, L. Jiao, J. L. Zhang, G. H. Cao, and H. Q. Yuan, *Phys. Rev. B* **91**, 220502(R) (2015).
- [43] A. Carrington and F. Manzano, *Phys. C (Amsterdam, Neth.)* **385**, 205 (2003).
- [44] A. Hillier and R. Cywinski, *Appl. Magn. Reson.* **13**, 95 (1997).
- [45] D. T. Adroja, A. D. Hillier, J.-G. Park, E. A. Goremychkin, K. A. McEwen, N. Takeda, R. Osborn, B. D. Rainford, and R. M. Ibberson, *Phys. Rev. B* **72**, 184503 (2005).
- [46] V. K. Anand, D. Britz, A. Bhattacharyya, D. T. Adroja, A. D. Hillier, A. M. Strydom, W. Kockelmann, B. D. Rainford, and K. A. McEwen, *Phys. Rev. B* **90**, 014513 (2014).
- [47] W. McMillan, *Phys. Rev.* **167**, 331 (1968).
- [48] C. Kittel, *Introduction to Solid State Physics*, 8th ed. (Wiley, New York, 2005).
- [49] Y. J. Uemura, G. M. Luke, B. J. Sternlieb, J. H. Brewer, J. F. Carolan, W. N. Hardy, R. Kadono, J. R. Kempton, R. F. Kiefl, S. R. Kreitzman, P. Mulhern, T. M. Riseman, D. L. Williams, B. X. Yang, S. Uchida, H. Takagi, J. Gopalakrishnan, A. W. Sleight, M. A. Subramanian, C. L. Chien *et al.*, *Phys. Rev. Lett.* **62**, 2317 (1989).
- [50] Y. J. Uemura, *Phys. C (Amsterdam, Neth.)* **185-189**, 733 (1991).
- [51] V. K. Anand, D. T. Adroja, and A. D. Hillier, Study of superconductivity in CaPd_2As_2 , SrPd_2As_2 and CaPd_2Ge_2 using muon spin relaxation and rotation, STFC ISIS Neutron and Muon Source, 2015, doi: [10.5286/ISIS.E.RB1510100](https://doi.org/10.5286/ISIS.E.RB1510100).